GRP SCHEMES FOR TIME-DEPENDENT 2-D AND QUASI 1-D FLOWS[1]

Matania Ben-Artzi and Joseph Falcovitz

Institute of Mathematics
Hebrew University of Jerusalem
Jerusalem 91904, Israel

ABSTRACT

The Generalized Riemann Problem (GRP) scheme for compressible time-dependent flows is briefly presented. A 2-D (Strang-type) operator splitting method that uses 1-D GRP as its basic building block is outlined. The 1-D Sod test problem and a 2-D cylindrical blast problem serve to demonstrate the high-resolution capabilities of GRP methods. Additional two-dimensional sample case are briefly considered. One with experimental validation of shock diffraction through double-bend conduit. Another with a comparison between fully two-dimensional solutions of wave interaction with area contraction segment in a duct, and the corresponding quasi one-dimensional approximation. The main thrust of the paper is in the validation, both analytic and experimental, of the quasi 1-D approximation and the operator splitting method, in the context of 2-D non-planar flows.

[1]Talk given by MBA at the Second Palestinian Mathematical Conference, Bet-Lehem, Palestine, August 2000.

1. INTRODUCTION

The Generalized Riemann Problem (GRP) scheme for time-dependent compressible flow in one space dimension, is a second-order accurate "analytic" extension to the classical (first-order accurate) Godunov scheme [7]. Over the past decade, aiming at practical simulation of shock wave phenomena, two-dimensional schemes (and most recently a three-dimensional one) were developed, using the GRP method as a fundamental building block.

This presentation is intended to serve as a concise introduction to the basic GRP methodology. For a more comprehensive account of the GRP method and its diverse applications, we recommend as a first reference the extensive review [5]. Further details of the GRP analysis and scheme may be found in earlier GRP publications [1,2].

The notion of "scheme extensions" is a central concept in regards to GRP methods. While we refer to [5] for an overview of major existing extensions, we shall mention them here briefly. For the treatment of multi-fluid shock wave phenomena a Material Interface Tracking (MIT) GRP extension was developed in two space dimensions. Another versatile 2-D GRP extension is the Moving Boundary Tracking (MBT) scheme, for flows involving moving/deforming boundary surfaces in a Cartesian grid. Diverse physical extensions were also introduced into the basic GRP method. A dusty gasdynamics scheme was developed by Wang and Wu [14], and more recently by Falcovitz and Igra [6]. Flows involving additional energy sources, such as chemical energy (combustion) and potential energy (self-gravity) were treated by adequately extended GRP schemes. Also, a "singularity tracking" (1-D) extension to the GRP method was employed for producing simulations of shock wave phenomena with near-perfect accuracy and resolution.

This presentation starts in Section 2 with an outline of the basic (one-dimensional) GRP method, followed by a computation of Sod's shock-tube problem [11] that demonstrates the accuracy and high-resolution of GRP simulation. In Section 3 the 2-D operator-split GRP scheme is outlined, followed by a cylindrical blast test problem. The good agreement between the 2-D simulation of that blast flow and the corresponding (cylindrically-symmetric) 1-D GRP simulation demonstrates the accuracy of the operator-split 2-D scheme. Here we also briefly consider two additional problems. One with experimental validation of shock diffraction through double-bend conduit. Another with a comparison between a fully two-dimensional solution of wave interaction with area contraction segment in a duct, and the corresponding quasi one-dimensional approximation.

It is emphasized that the purpose of this paper is not to review the (huge) existing literature concerning high-resolution (second-order) methods for nonlinear conservation laws. There is definitely no attempt at comparing features of different schemes. It is intended to give a rather self-contained review of the techniques used in the GRP approach (indeed, the multidimensional extension by operator-splitting is very classical and common to many methods), followed by a report on recent results related to quasi 1-D flows. Such flows (like spherically symmetric flows) are quite common in various physical and engineering settings. However, we feel that they are under-represented in the (high resolution) numerical literature. The test-cases mentioned here offer a "cross-examination" of the validity of

quasi 1-D high-resolution accuracy, on one hand, and its compatibility with full 2-D (split) calculations on the other hand.

2. OUTLINE OF THE GRP METHOD

A) Quasi 1-D Duct Flow Equations.

The equations governing the quasi-one-dimensional flow of an inviscid compressible fluid [4] through a duct having a smoothly varying cross-section area $A(r)$, as function of the space coordinate r and the time t are

$$A\frac{\partial}{\partial t}U + \frac{\partial}{\partial r}\left[AF(U)\right] + A\frac{\partial}{\partial r}G(U) = 0, \tag{2.1}$$

$$U(r,t) = \begin{pmatrix} \rho \\ \rho u \\ \rho E \end{pmatrix}, \quad F(U) = \begin{pmatrix} \rho u \\ \rho u^2 \\ (\rho E + p)u \end{pmatrix}, \quad G(U) = \begin{pmatrix} 0 \\ p \\ 0 \end{pmatrix}.$$

Here ρ, p, u, E are, respectively, density, pressure, velocity and total specific energy, where $E = e + \frac{1}{2}u^2$, e being the internal specific energy. In general, the thermodynamic variables p, ρ, e are related by an "equation of state". We shall frequently refer to the most common case, that of an ideal "γ-law" gas, where,

$$p = (\gamma - 1)\rho e, \qquad \gamma > 1. \tag{2.2}$$

B) Quasi-Conservative GRP Scheme.

The following notation is adopted for the finite-difference approximation to Eq. (2.1). The spatial grid is $r_i = i\Delta r, \quad i = 1, 2, ..., i_{max}$, where Δr is constant. The (numerical) solution is sought at equally spaced time-levels $t_n = n\Delta t$. By "cell i" we refer to the interval extending between the "cell-boundaries" $r_{i\pm\frac{1}{2}} = (i \pm \frac{1}{2})\Delta r$. We label by Q_i^n the average value of a quantity (flow variable) Q over cell i at time-level t_n. Similarly, $Q_{i+\frac{1}{2}}^{n+\frac{1}{2}}$ is the value of Q at the cell boundary $r_{i+\frac{1}{2}}$, averaged over the time interval (t_n, t_{n+1}). Flow variables are approximated as piecewise-linear in cells, where ΔQ_i^n denotes the "slope", i.e., the variation in Q over the $i-$cell interval. The discretization scheme is shown schematically in Fig. 1.

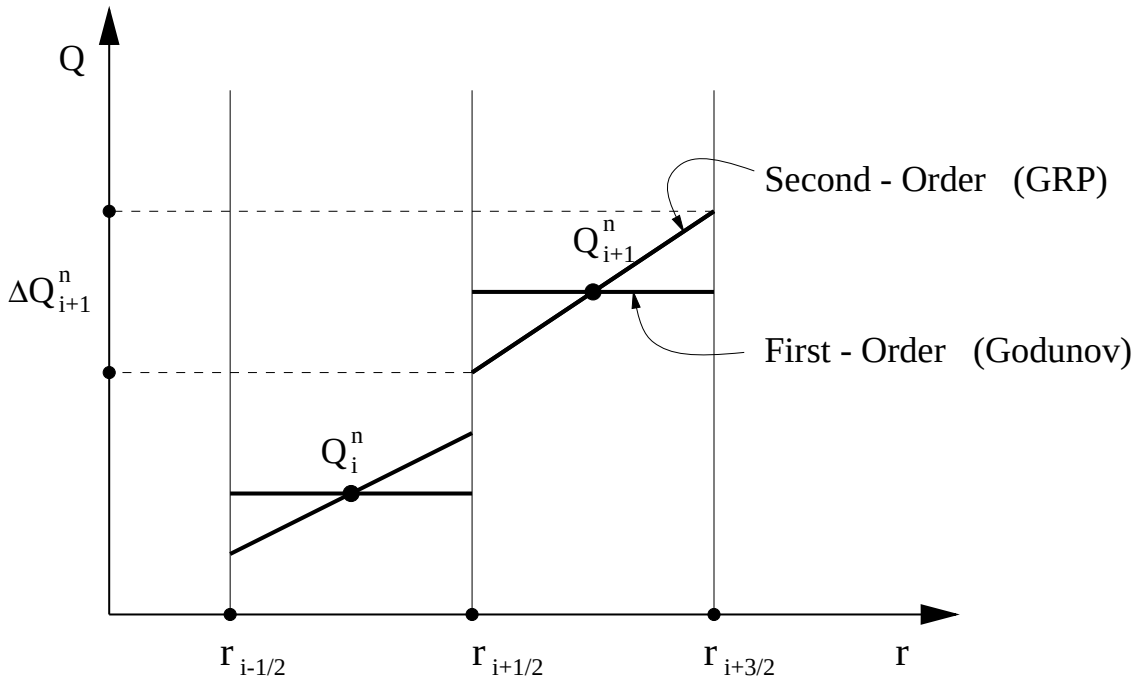

Figure 1. Distribution of Flow Variable per Cell

Taking the cell i to be a "finite-volume", a "quasi-conservative" difference scheme for (2.1) is given by

$$U_i^{n+1} - U_i^n = -\frac{\Delta t}{\Delta V_i}\Big\{ \Big[A(r_{i+\frac{1}{2}})F(U)^{n+\frac{1}{2}}_{i+\frac{1}{2}} - A(r_{i-\frac{1}{2}})F(U)^{n+\frac{1}{2}}_{i-\frac{1}{2}}\Big] + A(r_i)\cdot\Big[G(U)^{n+\frac{1}{2}}_{i+\frac{1}{2}} - G(U)^{n+\frac{1}{2}}_{i-\frac{1}{2}}\Big]\Big\}, \tag{2.3}$$

where $\Delta V_i = \int_{r_{i-\frac{1}{2}}}^{r_{i+\frac{1}{2}}} A(r)dr$ is the volume of cell i. The scheme (2.3) is completely defined only when the fluxes

$$F(U)^{n+\frac{1}{2}}_{i+\frac{1}{2}} = F(U^{n+\frac{1}{2}}_{i+\frac{1}{2}})\,, \qquad G(U)^{n+\frac{1}{2}}_{i+\frac{1}{2}} = G(U^{n+\frac{1}{2}}_{i+\frac{1}{2}})\,, \tag{2.4}$$

are specified as function of the "state variables" U_i^n and the respective slopes ΔU_i^n. It is emphasized that once U_i^{n+1} are evaluated by (2.3), they are never changed or modified in any way. The slopes of flow variables in cells are also updated to time-level t_{n+1}. They are, however, subject to monotonicity constraints [13], following the time-level updating. Here we will provide a sketch of the scheme, noting, in particular, the cases of the (first-order accurate) Godunov scheme, the (second-order accurate) GRP scheme and its simplified version E_1.

Godunov [7] proposed to solve (at every cell-boundary $r_{i+\frac{1}{2}}$) the "planar" **Riemann Problem** , obtained by solving Eq. (2.1) with $A(r) \equiv 1$ and piecewise-constant initial data consisting of the states U_i^n, U_{i+1}^n , on the left and right of $r_{i+\frac{1}{2}}$, respectively (see Fig.

1). The solution to a Riemann problem [4] is self-similar (as shown schematically in Fig. 2), so that $U_{i+\frac{1}{2}}^{n+\frac{1}{2}}$ for the flux in Eq. (2.4) is the solution at $r_{i+\frac{1}{2}}$ and $t - t_n = 0^+$. It is well known [10] that the resulting (first-order) scheme is stable and robust, but also that jump discontinuities are poorly resolved by it.

For the GRP scheme, the flow variable values $U_{i+\frac{1}{2}}^{n+\frac{1}{2}}$ for the flux in Eq. (2.4) are obtained by an analytic procedure based on solving at each grid point a **Generalized Riemann Problem** (GRP), which is the initial value problem for Eq. (2.1), having piecewise-linear initial data (see Fig. 1). The solution to a GRP is not self-similar (as shown schematically in Fig. 3), and the mid-step flow variables are evaluated from the following two-term Taylor expansion (in t).

$$U_{i+\frac{1}{2}}^{n+\frac{1}{2}} = U_{i+\frac{1}{2}}^{n} + \frac{\Delta t}{2} \cdot \left[\frac{\partial}{\partial t} U\right]_{i+\frac{1}{2}}^{n} . \tag{2.5}$$

The key idea of the GRP method is to derive the expressions for the mid-step fluxes analytically, according to Eqs. (2.4) and (2.5). This leads to a scheme where the fluxes are evaluated from plug-in expressions, thus constituting an "analytic" upgrading of the Godunov scheme to second-order accuracy level.

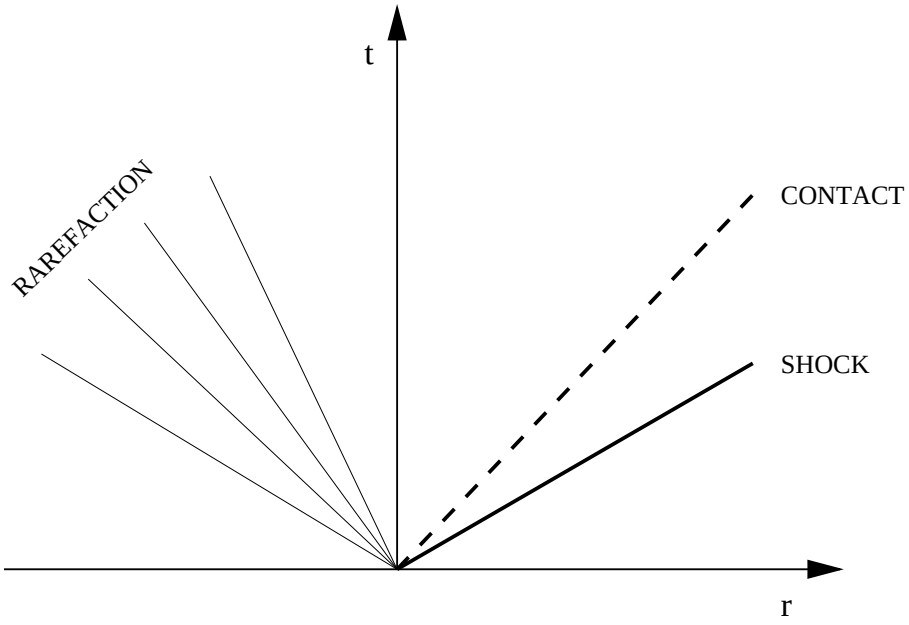

Figure 2. Self-Similar Solution to Riemann Problem

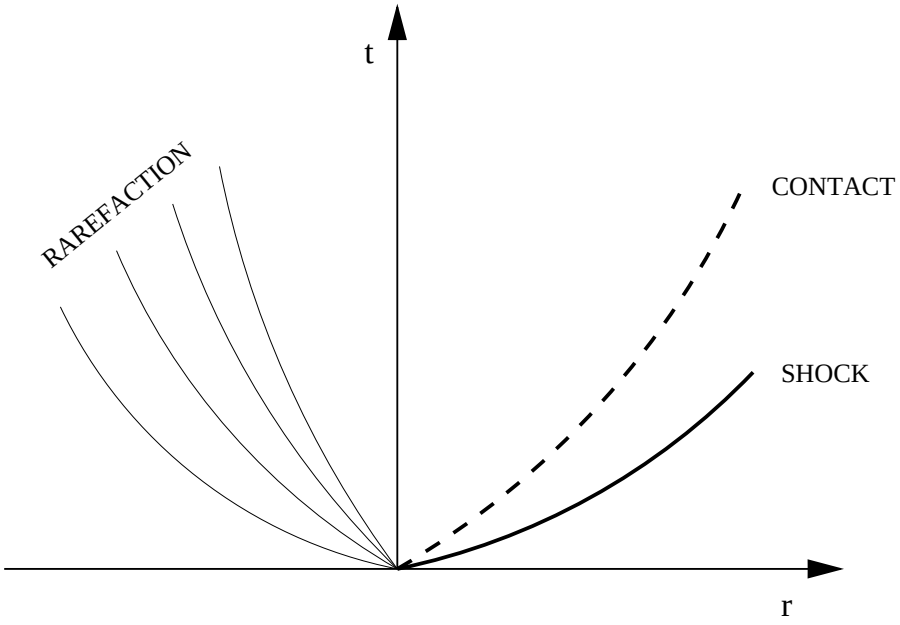

Figure 3. Solution to Generalized Riemann Problem

C) The E_1 Scheme.

By inspecting Eq. (2.5), it is clear that in order to get a second-order upgrading of Godunov's scheme, it suffices to determine the time-derivative with an $O(\Delta t)$ error, since then the error made in the evaluation of $U_{i+\frac{1}{2}}^{n+\frac{1}{2}}$ and the corresponding flux terms is of order $O(\Delta t^2)$. The resulting simplification denoted as the E_1 scheme, leads to an extremely simple modification of Godunov's scheme. Indeed, it is *the simplest possible modification that upgrades the Godunov scheme to a second-order accuracy level*. Our experience with numerous GRP computations indicates that in the vast majority of cases (i.e., in all regions of smooth flow), it suffices to use the simplified version. We actually wrote our GRP codes with both the simplified (E_1) and the "fully analytic" (E_∞) schemes, where the use of the latter is restricted to "difficult" grid-points (e.g., large jumps).

D) The Sod Shock-Tube Problem.

We now turn to the well-known shock-tube problem proposed by Sod [11] which has served as a standard test case for the evaluation of numerical schemes. The tube extends from $r = 0$ to $r = 100$ (with planar symmetry, $A(r) \equiv 1$) and is divided into 100 equal cells. The fluid is a γ-law perfect gas with $\gamma = 1.4$. The initial conditions are $u = 0$, $p = \rho = 1$ for $0 < r < 50$; $u = 0$, $p = 0.1$, $\rho = 0.125$ for $50 < r < 100$.

Two computations of that problem were performed, one using the Godunov scheme, the other with the GRP scheme. In Fig. 4 we show the flow profiles at $t = 20$ (the exact self-similar solution is given by the solid curve), obtained from the Godunov scheme. In Fig. 5 we show the same profiles obtained from the E_1/E_∞ GRP scheme. It is evident that both the contact and the shock discontinuities are far better resolved by the GRP scheme than by the Godunov scheme. The overall improvement due to the enhanced accuracy and high-resolution of the GRP scheme is quite dramatic.

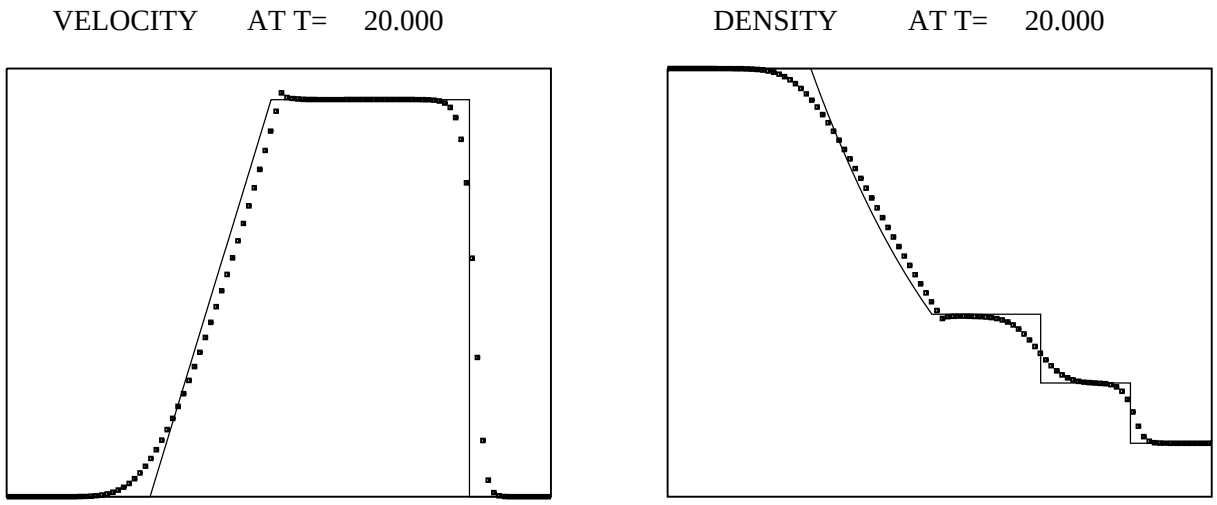

Figure 4. Sod's Shock-Tube problem. Godunov's method.

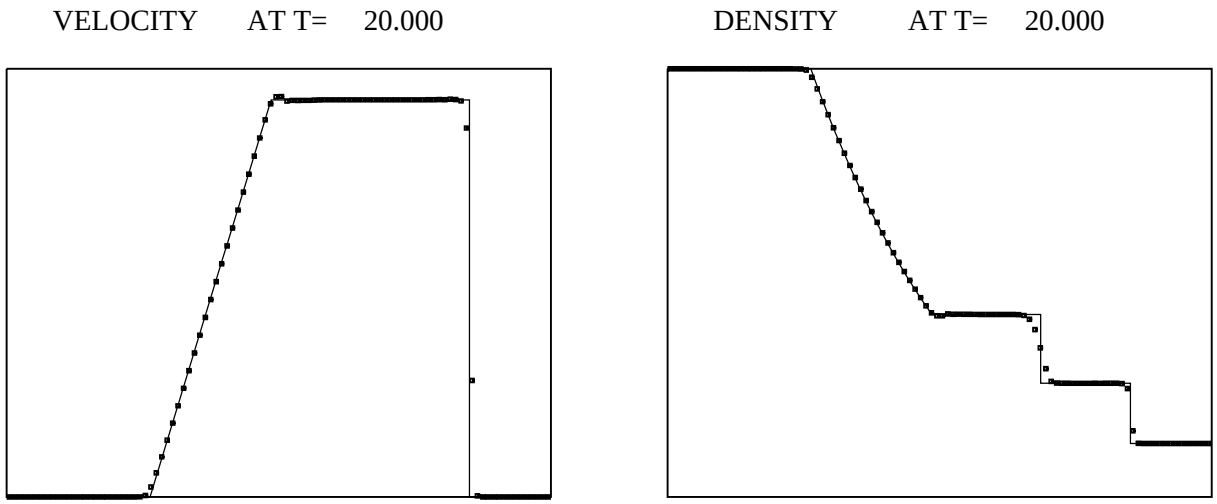

Figure 5. Sod's Shock-Tube problem. GRP method.

3. THE GRP METHOD FOR TWO-DIMENSIONAL FLOW

A) The Governing Equations.

Assuming an inviscid compressible fluid and an ideal gas equation of state, the time-dependent two-dimensional flow is governed by the laws for conservation of mass, momentum and energy, expressed in Cartesian coordinates (x, y) as

$$\partial_t U + \partial_x F(U) + \partial_y G(U) = 0,$$

$$U(x,y,t) = \begin{bmatrix} \rho \\ \rho u \\ \rho v \\ \rho E \end{bmatrix}, \quad F(U) = \begin{bmatrix} \rho u \\ \rho u^2 + p \\ \rho uv \\ u(\rho E + p) \end{bmatrix} \quad G(U) = \begin{bmatrix} \rho v \\ \rho uv \\ \rho v^2 + p \\ v(\rho E + p) \end{bmatrix}, \tag{3.1}$$

$$p = (\gamma - 1)\rho e, \quad \gamma = \text{constant } > 1, \tag{3.2}$$

$$e = E - \frac{1}{2}(u^2 + v^2). \tag{3.3}$$

In (3.1) we denote by ρ, p, e, E, u, v the density, pressure, specific-energy, specific total energy and (x, y)-velocity components, respectively.

B) Operator Splitting.

The two-dimensional finite-difference approximation to (3.1) is formulated as a "Strang-type" operator-splitting [12], using the GRP scheme as the one-dimensional finite-difference operator. This splitting procedure can be outlined as follows. The system (3.1) is first split into the two simpler systems,

$$\partial_t U + \partial_x F(U) = 0, \tag{3.4(i)}$$

$$\partial_t U + \partial_y G(U) = 0. \tag{3.4(ii)}$$

Loosely speaking, the system (3.4) is taken to mean that the evolution of an initial state U_o by (3.1) over a short time interval Δt, can be approximated by evolving U_o first subject to (3.4)(i) (over time Δt) obtaining a state U_1, then evolving U_1 in accordance with (3.4)(ii) again over time Δt.

Let $L_x(\Delta t)$, $L_y(\Delta t)$, $L(\Delta t)$ denote finite-difference approximation operators for the integration by a time-step Δt of (3.4)(i), (3.4)(ii), (3.1), respectively. Then, as shown by Strang [12], the operator sequence

$$L(\Delta t) = L_x(\frac{1}{2}\Delta t)L_y(\Delta t)L_x(\frac{1}{2}\Delta t) \tag{3.5}$$

is a second-order finite-difference approximation to (3.1).

The one-dimensional operators $L_x(\Delta t), L_y(\Delta t)$ are given by the planar "GRP solver". We reiterate the basic idea (in terms of L_x) as follows. The grid consists of the sequence of points $x_{i+1/2} = (i + 1/2)\Delta x,\ i = 0, 1, 2, \ldots, i_{max}$, where Δx is the grid spacing and cell i is the interval $x_{i-1/2} < x < x_{i+1/2}$. $U(x, y, t)$ (for a fixed y) is approximated at time $t = t_n = n\Delta t$ by $U^n(x, y)$, a piecewise linear distribution in cells, having the average value U_i^n in cell i. The finite-difference GRP solver L_x, yielding $\left\{U_i^{n+1}\right\}_{i=1}^{i_{max}}$ in terms of $\{U_i^n\}_{i=1}^{i_{max}}$ is explicitly given by,

$$U_i^{n+1} = U_i^n - \frac{\Delta t}{\Delta x}\left[F(U)_{i+1/2}^{n+1/2} - F(U)_{i-1/2}^{n+1/2}\right], \tag{3.6}$$

where the time-centered fluxes $F(U)_{i+1/2}^{n+1/2}$ are determined analytically from solutions to Generalized Riemann Problems that arise at the cell-interfaces $x_{i+1/2}$, as explained in Section 2(B) above.

C) Cylindrical Blast Example.

This sample problem was chosen to illustrate the capability of the two-dimensional GRP scheme, in a case where cylindrical symmetry permits also the application of the one-dimensional GRP scheme (2.3) with $A(r) = r$. A more detailed account of this problem is given in the recent publication [3]. The initial data is as follows. The fluid is an ideal gas having $\gamma = 1.4$ and it is initially at rest everywhere. Inside the circle centered at $(x, y) = (0, 0)$, of radius $R = 50$, there is a high-pressure state $(\rho_L, p_L) = (10, 20)$, while the low-pressure state outside the circle is $(\rho_R, p_R) = (1, 1)$. The computational domain is the square $(0 < x < 100, 0 < y < 100)$, which is divided into a grid of 100×100 square cells. The integration was carried out with a constant time-step $\Delta t = 0.16$, up to the final time of $T = 12.5$. Compliance with the Courant-Friedrichs-Levy (CFL) stability condition [10] throughout the computation was verified.

As a reference calculation, we used the quasi 1-D GRP scheme (2.3) to compute the flow profiles, as functions of the radial coordinate r. The pressure and density profiles thus obtained are shown in Fig. 6. They represent a sharp outgoing shock wave and an ingoing rarefaction, separated by a contact discontinuity.

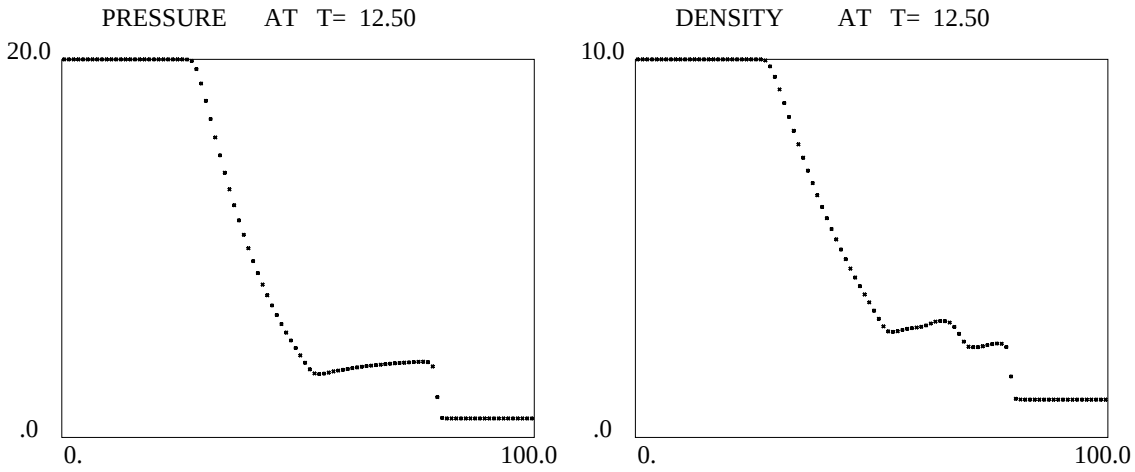

Figure 6. One-dimensional profiles as function of r

In the two-dimensional computation, the initial data in cells intersected by the circle was smoothed out, by taking an area-weighted density and pressure averages. The resulting density distributions are shown in Fig. 7(a) as a grey-scale plot (the amount of grey shading is proportional to the density), and in Fig. 7(b) as a diagonal cross-section (along the line $x = y$).

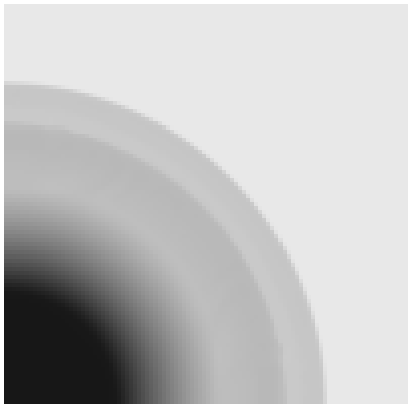

Figure 7(a). Density grey-scale plot on (x, y) plane, T=12.50.

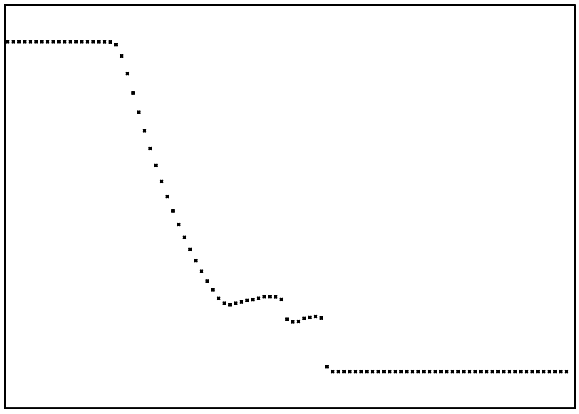

Figure 7(b). Density diagonal cross-section, T=12.50.

The agreement between the one-dimensional cylindrically-symmetric computations and the corresponding two-dimensional results is very good (compare the density profile in Fig. 7(b) with that of Fig. 6). This agreement underlines the fact that even though the schemes (2.3) and (3.5)-(3.6) are quite different in formulation, with the latter being based on operator-splitting, the results agree quite well.

D) Further Analysis of 2-D Flows.

Presently, two-dimensional fluid dynamical phenomena are accurately simulated by the GRP method, and additionally, experimental techniques for flow visualization are well developed. Thus, experimental validation of numerical computations is readily performed in two-dimensional setups. A number of two-dimensional sample cases were studied during the past decade, some with experimental validation and some without. Here we present summarily two such studies, referring to the original publications [8,9] for detailed accounts.

In a recent experimental and computational study of this kind [8], the diffraction of a shock wave propagating through a double-bend passage was visualized by shadowgraph and

double-exposure holographic methods. A notably good agreement was obtained between the experimental visualization and GRP computed results at a sequence of time points that covers the entire shock passing process [8].

In another study we considered the interaction of shock or rarefaction waves with a (smooth) contraction of the duct cross-sectional area [9]. Here the idea was to compare the fully two-dimensional solution with the corresponding one-dimensional approximation, obtained by solving numerically the quasi one-dimensional equations for compressible flow in a duct of varying cross-section area. The case of rarefaction wave propagating through an area contraction segment is shown in Fig. 8 as a time sequence of isobar maps. We note that at large time a stationary two-dimensional shock wave system, which appears to be a Mach reflection from the symmetry plane, has formed in order to match the pressure of the supersonic flow issuing from the narrow duct with the (higher) pressure prevailing downstream in the wider duct. Clearly this flow pattern is *inherently two-dimensional*, and cannot be approximated by a quasi one-dimensional duct flow. We refer to [9] for a more comprehensive analysis of this case.

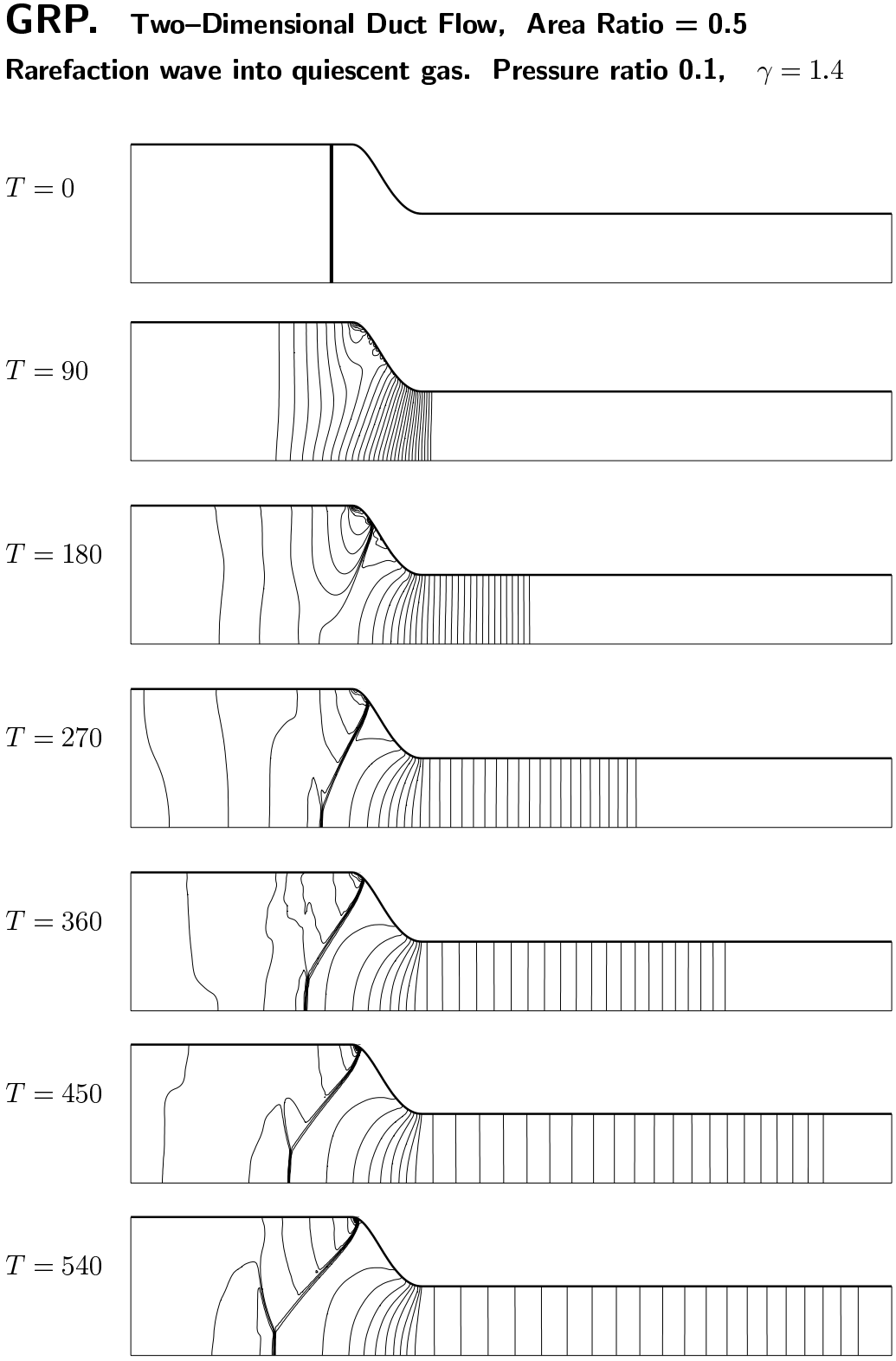

Figure 8. Isobars time-sequence of rarefaction wave interaction with area change.

4. References

1) M. Ben-Artzi and J. Falcovitz, A second-order Godunov-type scheme for compressible fluid dynamics, J. Comp. Phys. **55** (1984), 1–32.
2) M. Ben-Artzi and J. Falcovitz, An upwind second-order scheme for compressible duct flows, SIAM J. Sci. Stat. Comp. **7** (1986), 744–768.
3) M. Ben-Artzi, J. Falcovitz and U. Feldman, Remarks on high-resolution split schemes computation, SIAM Journal on Scientific Computing, **22**, 1008–1015, 2000.
4) R. Courant and K.O. Friedrichs, "Supersonic flow and shock waves", Springer–Verlag, New York 1976.
5) J. Falcovitz and M. Ben-Artzi, Recent Developments of the GRP Method, JSME International Journal, Series B, **38**, No. 4, 497–517, 1995.
6) J. Falcovitz and O. Igra, Analysis of Shock Wave Structure in Dusty Suspension, presented at the 14^{th} International Mach Reflection Symposium, Tohoku University, Sendai, Japan, 2–4 October, 2000.
7) S.K. Godunov, A finite difference method for the numerical computation of discontinuous solutions of the equations of fluid dynamics, Mat. Sbornik **47** (1959), 271–295.
8) O. Igra, J. Falcovitz, T. Meguro, K. Takayama and W. Heilig, Experimental and theoretical studies of shock wave propagation through double-bend ducts, Journal of Fluid Mechanics, **437**, 255–282, 2001.
9) O. Igra, L. Wang and J. Falcovitz, Non-stationary compressible flow in ducts with varying cross-section, Proc. Instn. Mech. Engrs., Part G, **212**, 225–243, 1998.
10) R.D. Richtmyer and K.W. Morton, "Difference Methods for Initial Value Problems", Interscience, New York 1967.
11) G.A. Sod, A survey of several finite difference methods for systems of non-linear hyperbolic conservation laws, J. Comp. Phys. **27** (1978), 1–31.
12) G. Strang, On the construction and comparison of difference schemes, SIAM J. Num. Anal. **5** (1968), 506–517.
13) B. van-Leer, Towards the ultimate conservative difference scheme V, J. Comp. Phys. **32** (1979), 101–136.
14) B.Y. Wang and R.S. Wu, Numerical investigation of dusty gas shock wave propagation along a variable cross-section channel, in "Shock Waves: Proc. of the 18th Int. Symp. on Shock Waves" (Ed. K. Takayama), Springer-Verlag 1991, pp. 521–526.